Chemosphere 311 (2023) 136926

Contents lists available at ScienceDirect

Chemosphere

journal homepage: www.elsevier.com/locate/chemosphere

Application of nano remediation of mine polluted in acid mine drainage water using machine learning model

Mingfei Ji [a,b,*], Bailian Li [c], Ali Majdi [d], Tamim Alkhalifah [e], Fahad Alturise [e], H. Elhosiny Ali [f,g,h]

[a] Collaborative Innovation Center of Water Security for Water Source Region of Mid-route Project of South-North Water Diversion of Henan Province, Nanyang Normal University, Nanyang, 473061, China

[b] College of Water Resource and Environment Engineering, Nanyang Normal University, Nanyang, 473061, China

[c] International Center for Ecology and Sustainability, University of California, Riverside, 17619 Glen Hollow Way, Riverside, CA, 92504, USA

[d] Department of Building and Construction Technologies Engineering, Al- Mustaqbal University College, 51001 Babylon, Iraq

[e] Department of Computer, College of Science and Arts in Ar Rass, Qassim University, Ar Rass, Qassim, Saudi Arabia

[f] Advanced Functional Materials & Optoelectronic Laboratory (AFMOL), Department of Physics, Faculty of Science, King Khalid University, P.O. Box 9004, Abha, 61413, Saudi Arabia

[g] Research Center for Advanced Materials Science (RCAMS), King Khalid University, P.O. Box 9004, Abha, 61413, Saudi Arabia

[h] Physics Department, Faculty of Science, Zagazig University, Zagazig, 44519, Egypt

HIGHLIGHTS

- PEI-DE particles' copper absorption level was examined by using synthetic and actual acid mine drainage samples at varied pH values.
- The findings of the copper uptake particles have been examined using several computational models.
- Using the n-fold 14 cross-validation approach, the quantities of parameters and C are estimated to be 0.001 and 0.01, SVM analysis was correct.
- Copper absorption of PEI-DE particles from synthetic and genuine acid mine drainage samples was studied under several pH conditions.
- Studies of filtering water at pH1 later confirmed that all of the adsorbed Cu was released.

GRAPHICAL ABSTRACT

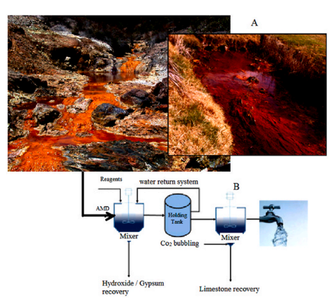

ARTICLE INFO

Keywords:
Polyethyleneimine particles (PEI)
Copper
Acid mine drainage (AND)
Water
Diatomaceous earth (DE)
Coal mines

ABSTRACT

Acid mine drainage (AMD) is the term used to describe drainage from coal mines with high sulfur-bearing rocks. The oxidative weathering of metal sulfides leads to AMD. The acidic environment corrodes more harmful compounds in the soil, which is spread throughout the working area. One such significant metal is copper, which is extracted in massive quantities from ores rich in sulfide. A copper-extraction resin might be created by combining diatomaceous earth (DE) particles with polyethyleneimine (PEI), which is shown to have great selectivity and affinity for copper. In this effort, PEI-DE particles' copper absorption level was examined by using synthetic and actual acid mine drainage samples at varied pH values. The findings of the copper uptake particles

* Corresponding author. Collaborative Innovation Center of Water Security for Water Source Region of Mid-route Project of South-North Water Diversion of Henan Province, Nanyang Normal University, Nanyang, 473061, China.

E-mail address: jimfdy@gmail.com (M. Ji).

https://doi.org/10.1016/j.chemosphere.2022.136926
Received 22 August 2022; Received in revised form 13 October 2022; Accepted 16 October 2022
Available online 19 October 2022
0045-6535/

Support vector machine (SVM)
Artificial intelligence

have been examined through the Support Vector Machine (SVM) model. Using the n-fold 14 cross-validation approach, the quantities of parameters and C are estimated to be 0.001 and 0.01, respectively. The SVM analysis was correct, and the findings indicated that copper could bind to the material efficiently and preferentially at pH 4. Subsequent water elution studies at a pH value of 1 confirmed the pH-reliant interaction between dissolved Cu and PEI by demonstrating full release of the adsorbed Cu. In this research, the copper absorption of PEI-DE particles from synthetic and genuine AMD specimens was studied based on several pH conditions. The findings suggest that copper may attach to the material effectively and preferentially at pH 4. Studies of filtering water at pH1 later confirmed that all of the adsorbed Cu was released. This shows that the interaction between PEI and dissolved Cu depends on PH.

1. Introduction

Acid mine drainage (AMD) refers to the environmental pollution (Pan and Chen, 2021; Dai et al., 2022), particularly aquatic bodies, by the drainage of water from locations including sulfur-bearing minerals. This is a serious problem nowadays. Even though AMD may occur naturally, human activities as the processing of metal coal and mining can contribute considerably to its creation on a wide scale (Johnson and Hallberg, 2005; Chahnasir et al., 2018; Arabnejad Khanouki et al., 2010a). Mining exposes sulfide minerals to the environment, leading to the production of an excessive quantity of acid that may have both immediate and long-term harmful consequences for the ecosystem. Acid mine drainage has remained a significant environmental problem. Metal mining is one of the biggest environmental problems that needs to be dealt with (Kleinmann, 1985; Pierson-Wickmann et al., 2011; Rezania et al., 2017; Ge et al., 2019). AMD has a lot of negative impacts, such as destroying the quality of the soil and causing mining equipment and machinery to rust (Gaikwad and Gupta, 2008; ; ;). It also hurts the ecosystems of the streams that get the drainage water and pollutes the groundwater by letting heavy metals leach out of the acid mine water (Adler and Rascher, 2007; Kamyab et al., 2014a, 2016a; Guan et al., 2021). Acid mine drainage water has been linked to both environmental and health problems (Lin et al., 2022; Abdullah et al., 2022; Vadivelu et al., 2020; Chelliapan et al., 2020). Additionally, attempts have been done to highlight the application of two emerging techniques (phytoremediation and Nanoremediation (Kleinmann, 1985)) together (Bai et al., 2022; Liu et al., 2008). A hypothetical model was developed in which hyperaccumulator plants might be trained to improve their phyto-remedial capacity for the effective treatment of mine-polluted water. When exposed to water or air, sulfide-containing minerals such as iron disulfide or iron pryrite undergo natural oxidation, resulting in AMD (Putri et al., 2011; Kamyab et al.; Vasseghian et al., 2022; Kamyab et al., 2016b). In addition to natural processes, human activities as mining and building expose the earth's surface, result in acidic drainage. The interaction between oxygen, water and metal sulfides produces metal sulfates and sulfuric acid. Metals may be further oxidized to enhance acidity (Banfield and Nealson, 2018; Banfield, 1997; Rezania et al., 2019; Roudi, 2014; Ilmasari et al., 2022). Water enters the mines as fresh water, either as precipitation or as water utilized for drilling, dust control, and other mining processes. There is always the possibility of groundwater seepage into underground mines via cracks and fissures (Hubicki and Kołodyńska, 2012; Anita et al., 2014; Abd Majid et al., 2015a; Kamyab et al., 2016c). The oxidized products of sulfide minerals are carried by water into the surrounding water, where they may then be carried to nearby rivers and other bodies of water (Singh, 1987; Yang et al., 2022; Abd Majid et al., 2015b; Ahmad et al., 2016). In a variety of sectors, including pharmaceuticals, mineral and mining processing, food, manufacturing, power and fuel, wastewater and water treatment, and agriculture, the optimized removal of dissolved metal ions and species from water solutions is an insurmountable issue (Hubicki and Kołodyńska, 2012; Sharma et al., 2022; Azizan et al., 2022a). For instance, there are techno-economic restrictions on the use of standard division and/or purifying procedures to address hazardous or heavy metal water contamination caused by industrial, mining, agricultural, and chemical waste disposal operations (John, 2002; Duffus, 2002; Kamyab et al., 2022a; Michael et al., 2022; Balaraman et al., 2020). As an alternative, less costly mesoporous and naturally occurring materials like diatomaceous earth (DE) particles are drawing significant interest (Iiyama et al., 2004; Setia et al., 2021; Krishnan et al., 2021; Selvama et al., 2019; Yu et al., 2012; Azizan et al., 2022b). These materials have high metal ion sorption capacities comparable to the high-cost synthetic adsorbents. The most appealing characteristics of DE particles are their low cost, abundance in nature, and distinctive and complex structural, mechanical, and chemical features. The current, rapidly expanding interest in its use for water filtration is also due to the result of these fundamental properties (Iiyama et al., 2004; Bariana et al., 2013; Rezania et al., 2022). For instance, it has been studied how varied circumstances (such as heat and pH) affect the adsorption of organic pollutants and heavy metal ions onto unaltered and modified DE particles from aqueous solutions. Studies on the removal of Cr (III) ions and U(VI) from aqueous solution by functionalized and unfunctionalized DE particles revealed that the former's adsorption capability was significantly improved (Alothman and Apblett, 2010; Wang and Smith, 2007; Cheah et al., 2018; Qureshi et al., 2022a; Liu et al., 2020). According to Gao et al. (2005), PEI-functionalized DE particles demonstrated an extremely potent phenol-trapping effect in neutral aqueous solution by combining strong electrostatic and hydrogen bonding interactions. Numerous investigations into the DE material on Cu adsorption and heavy metals (i.e., mercury, chromium, and nickel) from water systems have been conducted to date (Iiyama et al., 2004; Aivalioti et al., 2012; Qureshi et al., 2022b; Zain et al., 2022). The utilization of copper for cutting-edge marine applications as well as the treatment of copper-contaminated marine habitats may both be made possible by materials that can bind copper from saltwater (Shu et al., 2021; Shi et al., 2020; Shah et al., 2016a). Copper pollution in marinas may come from the anti-biofouling coatings on boats, and tributyltin (TBT) free anti-biofouling coatings might follow the same rules (Lindén et al., 2015; Awual et al., 2013; Schiff, 2004; Esfahan et al., 2020; Oryani et al., 2022). So far, the industrial and academic groups studies on anti-biofouling coatings are not able to come up with new environment friendly alternatives and don't use biocides, but work as the coatings and release copper. A method for preventing biofouling that uses the accumulation and release of copper, which is normally found in large amounts in water, to create a biocidal flux of copper across an interface, such as a coating, without putting any copper into the water (Arabi--Nowdeh et al., 2021). The method uses polymers that are selective for copper for uptake and polymers that conduct electricity and are active for triggering release. It has four steps: 1) copper is taken up by the coating, 2) an electrochemical stimulus starts the coating to release copper, 3) the released copper prevents biofouling, and 4) an electrochemical stimulus switches the coating back to copper-uptake mode. Copper can always be found in saltwater, so this would make it possible for a cycle that never ends. A variety of AMD treatment methods were created to date depending on biological, physical, and chemical processes, either in combination or alone. Systems are often divided into "active " or "passive" categories based on the procedure (Taylor et al., 2005; Sheoran and Sheoran, 2006; Milovančević et al., 2019; Azizan et al. Kamyab; Shah et al., 2016b). Processes including ion exchange,

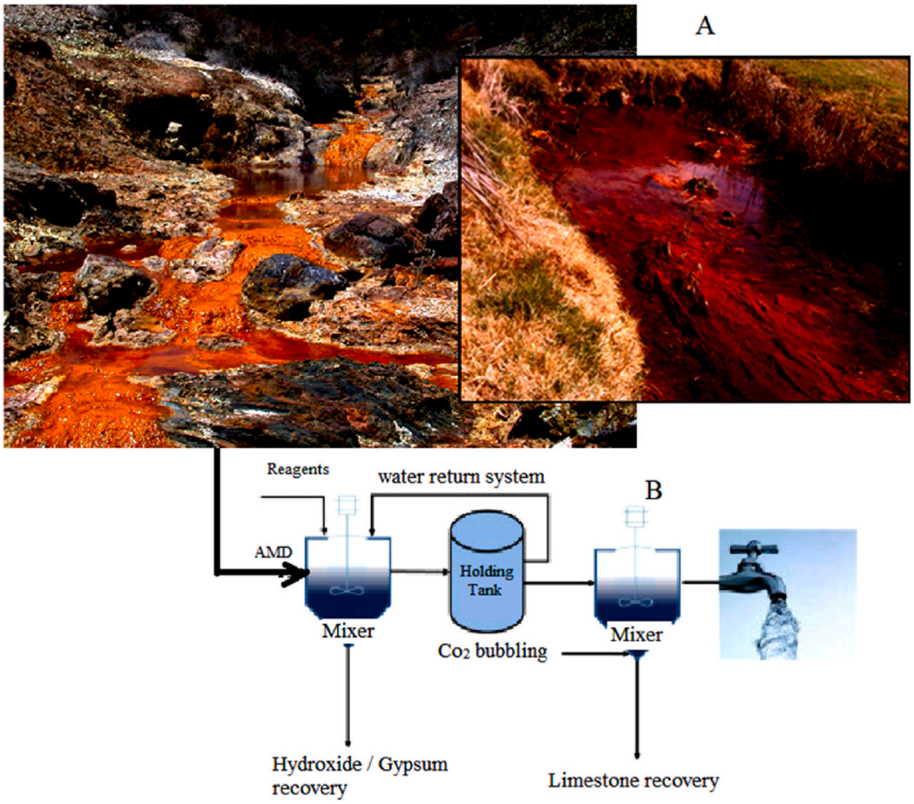

Fig. 1. Treatment of acid mine drainage (AMD) (a). The treatment process comprises three steps which include neutralization, using magnesite, gypsum synthesis, using lime and limestone synthesis, using CO_2 bubbling. Few parameters as structure, flow direction, and size differ among reactors, however, passive systems include at least two biotic procedures: sulfate decline to H_2 sulfide pollution with organic compounds' oxidation and breakdown of polymeric organic matter into low-molecular weight organic compounds (b).

electrochemical concentration, precipitation or PH regulation, redox control (sulfate reduction), absorption, biological mediation, flocculation/filtration/settling and crystallization are examples (Taylor et al., 2005; Sheoran and Sheoran, 2006; Akinwekomi et al., 2016; Zhang et al., 2016; Yadav et al., 2022; Shariati et al., 2021a; Kamyab et al., 2022b). The key distinction among these treatment methods is how well they can handle the flow rate, acidity, and acidity load of the influent AMD (Taylor et al., 2005; Kamyab et al., 2014b, 2014c,). The most frequent and inexpensive approach utilized is pH control via low cost neutralizing reagents (such as pervious concrete, limestone) (Shabalala et al., 2017; Offeddu et al., 2015, 2014; Zainah and Shahaboddin, 1801; Shariati et al., 2020a). Because of its considerable long-term environmental and economic effects, AMD continues to provide a serious challenge to the environmental and mining industries (Taylor et al., 2005; McCarthy, 2011; Jamal et al., 2015) despite numerous researches on the development of various solutions for treatment. For example, one of the most frequent sources of metal contamination in freshwater is mining activity in general and AMD in particular (Shariati et al., 2011a). The ease of sulfide minerals' oxidation toward the generation of acid leads to contaminated wastewater in many mine sites. Acid relates to the overburden or waste deposit while there are no calcareous materials (Rezania et al., 2018; Ashokkumar et al., 2019; Khoshnava et al., 2020). Acid rock drainage (ARD) might have a high amount of sulfate, iron and base metals as zinc, lead, copper, silver, nickel, or based on the constituents of the waste, and shows pH ratios totally below 7. Considering the lack of an obvious view of the initial pyrite oxidation process, ARD generation is defined as a complex process, including solid–solution equilibria, complexation and hydrolysis reactions, and a few oxidation–reduction reactions. Thus, the real ARD generation reactions are both chemical and involve some biochemical or biological impacts that add to the vagueness of the process (Shariati et al., 2019a; Yavari et al., 2022; Hosseini et al., 2019). Despite many works on ARD formation, ARD still is a major surrounding concern in terms of the mineral and mining industry. ARD has the repeated treatment and collection of the generated acidic effluent (Velu et al., 2021; Shariati et al., 2012a). Regardless of its high cost and ineffectiveness, this method needs an indefinite period of treatment sludge disposal and treatment facilities because acid generation might last for decades following mine closure. Except for a few, the majority of studies focus on effluent treatment enhancement systems rather than controlling ARD formation at the source. The use of chelating diamines to remove copper from tainted natural waters was effectively shown by Chouyyok et al. (2010). In terms of mining the oceans, it should be noted that polymer-based materials have received the majority of attention based on the Schwochau's critical evaluation (Schwochau, 1984), but this process requires high energy (Bardi, 2010). Polyethyleneimine (PEI)-based materials were highly studied for metal binding (Duru et al., 2001). Fe^{2+}, Co^{2+}, Zn^{2+}, Ni^{2+}, Hg^{2+}, Cr^{3+}, Cd^{2+}, Pb^{2+}, and Cu^{2+} has been demonstrated as the removal ions from waste waters (Pang et al., 2011) with a strong preference for copper (Pang et al., 2011; Beatty et al., 1999; Prasad et al., 2020; Soltani et al., 2013). PEI is often attached to carrier particles, such as poly (methyl methacrylate) microspheres (Maketon and Ogden, 2008; Steinmann et al., 1994), porous cellulose material (Chanda and Pillay, 2005), silica powder (Deng and Ting, 2005a), porous magnetic agarose beads (Deng and Ting, 2005b), commercial acrylic fiber (Chanda and Pillay, 2005), agarose beads, and polystyrene-based macroporous cation exchange resin (Chanda and Pillay, 2005). Fig. 1 shows AMD treatment.

Sulfuric acid and iron sulfate are produced primarily as a result of reactions between oxygen, water, and pyritic sulfur. This kind of situation often occurs in coal mines, and the resulting acidic environment encourages the development and activity of several *acidophilic bacteria*, including *Thiobacillus ferroxidans*. The *bacterium* speeds up the acid-making reaction and makes it happen highly faster than chemical oxidation, which makes the water more acidic (Singh and Bhatnagar, 1985; BridgeHallberg, 2005; Shariati et al., 2020b, 2020c). The hydrolysis of oxidized pyrite products and the production of sulfuric acid are the two key factors that control how acidic the mine drainage water is. In contrast, the sulfur content aids in determining how much reactive

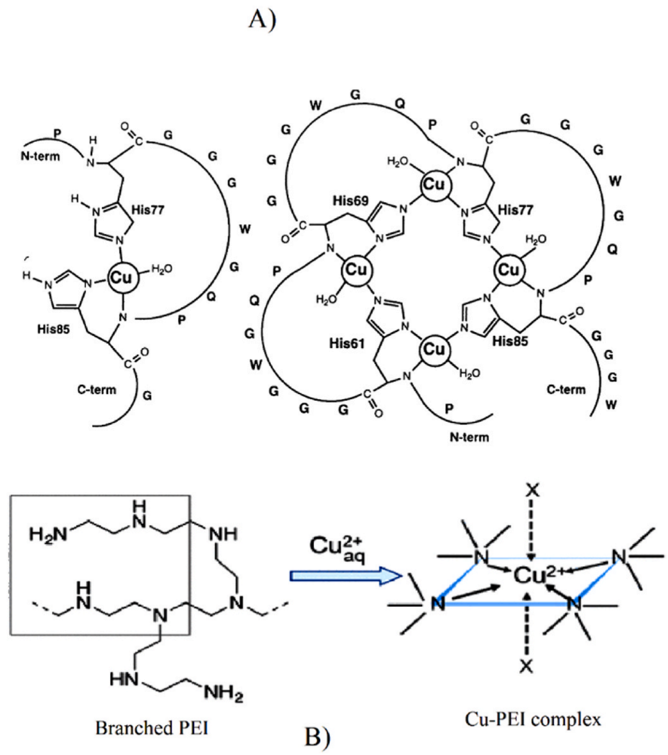

Fig. 2. The copper-binding design is shown schematically (resting oxidized state). It has been shown that the copper-binding capability of the PEI materials is higher than that of the original microgel (A). Compared to the microgel particles and original composites, the copper-binding behavior of etched (PEI-free) materials indicates that nano-particles within the composite raise the copper-binding sites' number in PEI system instead of directly absorbing copper (B).

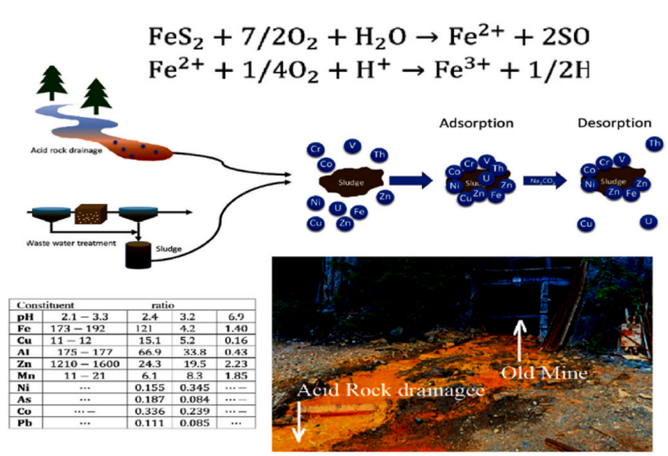

Constituent	ratio			
pH	2.1 – 3.3	2.4	3.2	6.9
Fe	173 – 192	121	4.2	1.40
Cu	11 – 12	15.1	5.2	0.16
Al	175 – 177	66.9	33.8	0.43
Zn	1210 – 1600	24.3	19.5	2.23
Mn	11 – 21	6.1	8.3	1.85
Ni	···	0.155	0.345	··· —
As	···	0.187	0.084	··· —
Co	··· —	0.336	0.239	··· —
Pb	···	0.111	0.085	···

Fig. 3. Utilizing waste digested activated sludge, metal ions from acidic multi-metal mine water are removed and recovered. Properties of acid mine drainage (lower Table) and the acidic water (lower figure).

pyrite is present in a certain stream (Singh, 1987). Fig. 2 shows the schematic of the copper-binding design.

First, water and oxygen in the air react with ferrous sulfide (pyrite) to make ferrous sulfate and sulfuric acid.

$$FeS_2 + H_2O + 3\frac{1}{2}O_2 \rightarrow FeSO_4 + H_2SO_4 \tag{1}$$

Ferric sulfate gets dissolved in the acidic water.

$$FeSO_4 \rightarrow Fe_2(SO_4)_3 \rightarrow 2Fe^{3+} + 3SO_4^{-2} \tag{2}$$

Upon coming into contact with water, Fe^{3+} may undergo a hydrolysis reaction, forming ferric hydroxide and releasing hydrogen ions in the process. The hydrogen ions cause the acidity of water to rise.

$$Fe^{3+} + 3H_2O \rightarrow Fe(OH)_3 + 3H^+ \tag{3}$$

Fig. 3 shows that by utilizing waste digested activated sludge, metal ions from acidic multi-metal mine water are removed and recovered. The majority of the waste produced by industrial activity worldwide is comprised of tailings, which are produced by mineral processing and mining facilities (Kagambega et al., 2014; Lottermoser, 2010; Krishnan et al., 2022; Othman et al., 2021). Although there is a lack of precise information on mine waste production, some estimates indicate that 20–25 million tons of solid mine waste are generated annually globally (Sheoran and Sheoran, 2006; Kagambega et al., 2014; Nor et al., 2022; Soni et al., 2022; Al-Dailami et al., 2022). One of the unintended effects of coal and metal mining operations is the discharge of acidic water from certain mine wastes as AMD illustrated in Equations (4)–(7), when residual sulfide minerals like pyrite are oxidized with water, *bacteria* and air (oxygen) to release protons of (H^+) and hence reduce pH (Jennings et al., 2008; Kokila et al., 2021). Some of these processes (Eq. (5), (6), and (7)) are termed to be catalyzed by Fe and sulfur-oxidizing *bacteria* at low pH, boosting the rates of reactions by many orders of magnitude (Jennings et al., 2008; Nordstrom and Southam, 1997; Yazdani et al., 2021).

$$2FeS_2(s) + 2H_2O + 7O_2 \rightarrow 2Fe^{2+} + 4H^+ + 4SO_4^{2-} \tag{4}$$

$$2Fe^{2+} + \frac{1}{2O_2} + 2H^+ \rightarrow H_2O + 2Fe^{3+} \tag{5}$$

$$6H_2O + 2Fe^{3+} \leftrightarrow 6H^+ + 2Fe(OH)_3(s) \tag{6}$$

$$14Fe^{3+} + FeS_2(s) + 8H_2O \rightarrow 2SO_4^{2-} + 16H^+ + 15Fe^{2+} \tag{7}$$

1.1. AMD chemistry

The total oxidation of pyrite is a complicated procedure which include a variety of products and reactants under different sates. The pyrite oxidation caused by exposure to air has been extensively studied and is described by Equations (8) and (9) (Simate and Ndlovu, 2014; Black and Craw, 2001; Bwapwa et al., 2017). As shown in the formula, the oxidation of pyrite by oxygen in the presence of water is the initial step in the weathering of pyrite (1). Ferrous iron is liberated when sulfur is oxidized to sulfate. For every mole of pyrite that is oxidized, this process makes 2 mol of acid.

$$2FeS_2 + 2H_2O + 7O_2 \rightarrow 2Fe^{2+} + 4H^+ + 4SO_4^{2-} \tag{8}$$

$$\text{Pyrite} + \text{Water} + \text{Oxygen} \rightarrow \text{Ferrous Iron} + \text{Acidity} + \text{Sulfate} \tag{9}$$

The rate-controlling step is the oxidation of ferrous ions to ferric ions. One mole of acid is used for every mole of ferrous ions present. Certain *bacteria* accelerate this pH-dependent chemical process. Under acidic circumstances (pH between 2 and 3) and in the absence of microorganisms, the process proceeds slowly. Nevertheless, at a pH of ~5, the reaction ratio is quicker. The response is

$$4Fe^{2+} + 4H^+ + O_2 \rightarrow 2H_2O + 4Fe^{3+} \tag{10}$$

After that, iron undergoes hydrolysis, causing the water molecule to break and producing additional acid. Ferric hydroxide is precipitated above pH 3.5. Ferric hydroxide precipitate (solid) production is pH based. If the pH is more than ~3.5, solids are developed; but at pH 3.5 or below, little to no solids are precipitated.

$$2Fe^{3+} + 6H_2O \rightarrow 2Fe(OH)_3\downarrow + 6H^+ \tag{11}$$

Water + Ferric Iron → Acidity + Ferric Hydroxide (yellowboy).

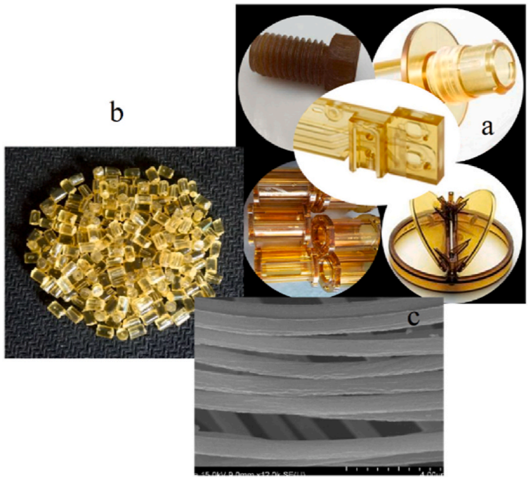

Fig. 4. Polyethyleneimine particles (a), application of polyethyleneimine particles (b), SEM of a PEI-DE particle after equilibrium Cu uptake (c).

Later, Ferric iron could oxidize more pyrite in a fast and continues reaction until the depletion of pyrite or ferric iron.

$$FeS_2 + 8H_2O + 14Fe^{3+} \rightarrow 2SO_4^{2-} + 15Fe^{2+} + 16H^+ \tag{12}$$

Pyrite + Water + Ferric Iron → Acidity + Sulfate + Ferrous Iron Accordingly, significant acid is gained by the overall reaction.

$$4FeS_2 + 15O_2 + 14H_2O \rightarrow 8H_2SO_4 + 4Fe(OH)_3\downarrow \tag{13}$$

$$\text{Pyrite} + \text{Water} + \text{Oxygen} \rightarrow \text{Sulfuric Acid} + \text{''Yellowboy''} \tag{14}$$

$$CuS + O_2 + H_2O \rightarrow Cu^{2+} + SO_4^{2-} + H^+ \tag{15}$$

The metals contained in other minerals may then be released by dissolving them with this acid. Cu is one of the main metals released by this process, having risk parameters that prevent its entering to the environment.

1.2. Significance of study

Due to its considerable long-term and economic environmental effects, AMD continues to provide a serious challenge to the environment and mining industry (Taylor et al., 2005; McCarthy, 2011; Jamal et al., 2015) despite numerous researches on the development of various solutions for treatment. For example, one of the most frequent sources of metal contamination in freshwater is mining activity in general and AMD in particular. The primary goals of this research are to describe the copper binding of PEI-DE nanoparticles and to look into the removal and selective recovery of Cu from freshwater contaminated with AMD. To accomplish this, PEI-DE particles were examined for copper extraction from model AMD-relevant solutions, and the effectiveness was shown in a real solution. Support vector machine analysis (SVM) has also been used to look into the copper uptake particles' results (Shariati et al., 2021b; Soni and Das, 2022). Fig. 4 shows Polyethyleneimine particles.

1.3. PEI of copper complex

Free Cu^{2+} significantly raised the conductivity of the solution in Fig. 7a as the Cu^{2+} concentration in the 10 mM PEI solution was raised till all chelation sites were used. In contrast, Fig. 7b shows that as the PEI content rises, the conductivity of the 1 mM $CuSO_4$ solution reduces till all Cu^{2+} is bound. The ratio of chelation between the Cu and PEI amino groups may be calculated in both situations by looking at the point at which the slope of the curve varies. In both circumstances, this ratio is 0.25 for the PEI/Cu ratio or 4. The process in eq. (4) shifts to the left, lowering pH, and due to the positive charges, the PEI/Cu could attract anions (OH^- in Eq. (16)), due to the use of un-protonated amino groups by Cu^{2+}

$$4PEI + Cu^{2+} \Leftrightarrow 4PEI - Cu^{2+} \tag{16}$$

$$4PEI - Cu^{2+} + 2H_2O \Leftrightarrow 4PEI - Cu^{2+} - 2OH^- + 2H^+ \tag{17}$$

In recent years, Artificial Intelligence (AI) technique has been widely used in various applications (Zhao et al., 2020a, 2020b, 2021, 2021; Zhao et al., 2021; Foong et al., 2021; Liu et al., 2021). The capability of AI has been indicated in many studies compared to other numerical methods (Marynirmala and Sivakumar, 2021; Arora et al., 2021; Eyo

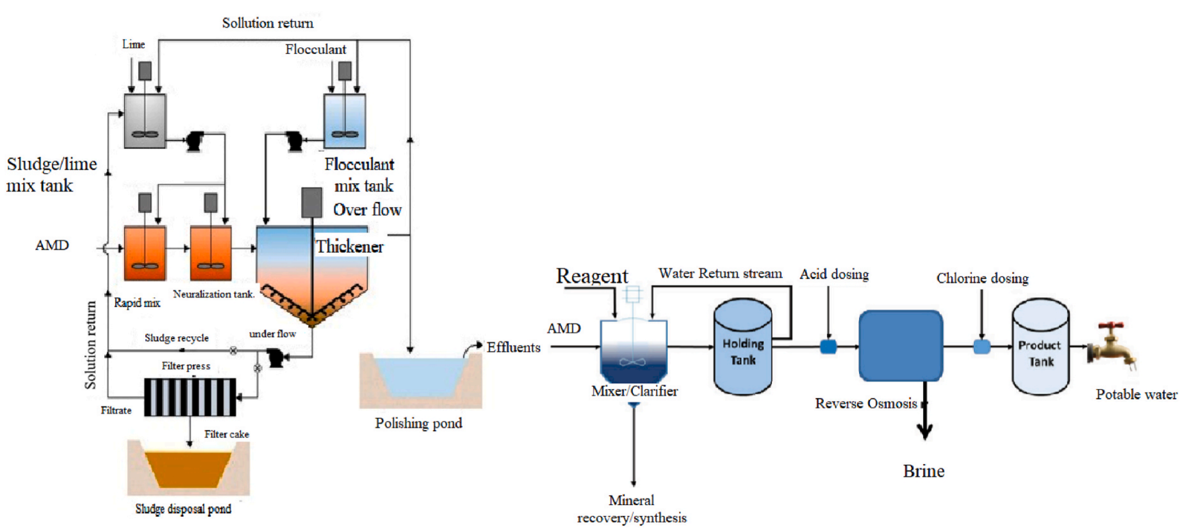

Fig. 5. Schematic presentation of acid mine drainage treatment process. In order to recover important minerals of economic worth and to provide water suitable for a wide range of specified uses, including irrigation, drinking, and industrial applications, lime, calcined cryptocrystalline magnesite, and soda ash were used. AMD from coal mining procedures was employed in the mineral recovery, synthesis, and water reclamation processes. In the first reactor, metal hydroxides were formed using a sequential and fractional precipitation method. Passive systems may be successfully applied under low-flow and low-acidity conditions as a single long-term fix for numerous AMD issues. Passive systems might still be suitable when flow or acidity concentrations are minimal, providing that they are properly built and maintained.

Table 1
Correlation matrix between Cu and heavy metals ratio.

	pH	SO_4	Cl	HCO_3	Ca	Mg	Cu	Fe
pH	1							
SO_4	− 0.711	1						
Cl	− 0.041	− 0.015	1.					
HCO	0.340	− 0.407	0.5 23	1				
Ca	− 0.311	0.635	0.0 14	−0.01 3	1			
Mg	−0.6 48	0.622	−0.00 3	− 0.222	0.101	1		
Cu	−0.6 12	0.618	− 0.121	− 0.11	0.268	0.712	1	
Fe	0.001	0.065	− 0.175	−0.2 19	−0.1 35	−0.00 4	− 0.072	

Table 2
SVM's optimum value and training range parameters.

Parameter	Min	Max	Step	Optimize
A	0.01	6	0.01	0.001
C	0.1	11	0.01	0.01

Table 3
R^2 and RMSE of SVM in train and test data.

Method	R_1	R_2	RMS_1	RMS_2
	Cu	Cu	Cu	Cu
SVM	0.933	0.936	0.543	0.466

Table 4
Composition of acid mine drainage.

Constituent ratio				
pH	2.1 – 3.3	2.4	3. 2	6.9
Fe	173 – 19 2	121	4. 2	1.40
Cu	11 – 1 2	15.1	5. 2	0.16
AI	175 – 177	66.9	33.8	0.43
Zn	1210 – 1600	24.3	19.5	2.23
Mn	11 – 21	6.1	8.3	1.85
Ni	…	0.155	0.345	… –
As	…	0.187	0.084	… –
Co	… –	0.336	0.239	… –
Pb	…	0.111	0.085	…

et al., 2022; Bulut and. Özceylan, 2021; Teimoori et al., 2021; Babaee Khobdeh et al., 2021). Many classification techniques can be divided into unsupervised and supervised categories (Duda and Hart, 2006; Duda et al., 1973; Shariati et al., 2011b, 2012b; Arabnejad Khanouki et al., 2010b). SVM has gained a lot of popularity recently and has been broadly utilized, comprising of classification and regression among others (Maslahati Roudi et al., 2018; Karimi et al., 2016; Nilashi et al., 2019; Hosur Shivaramaiah et al., 2022). The SVM method has also been proved successful in mineral and mining exploration. For example, land cover classification (El-Khoribi, 2008; Shariati et al., 2019b, 2020d), alteration zones (Abbaszadeh et al., 2013), potential mineral mapping (MPM), and separation, multi-classes problems (Zuo and Carranza, 2011; Zhao and Foong, 2022; Zhao and Wang, 2022; Zhao et al., 2020c, 2022; Yan et al., 2019). The porphyry copper deposit (the world's greatest source of copper) is distinguished by low grades and high tons of ore mineralization. It may also be a source of molybdenum and gold (Richards, 2003). As a result, a lot of researchers have looked at porphyry Cu deposits. For instance, changing mapping for porphyry Cu deposits is created using data from remote sensing satellites (Safari et al., 2018; Shariati et al., 2020e). By assessing the preciseness ratio on the SVM efficiency, the impacts of the input characteristics are assessed in this research. Finally, the radial basis function (RBF) is used as a kernel function, and lithology, alteration, mineralization, level, and other input characteristics are used to create the SVM model. Additionally, using the n-fold cross-validation approach, the ideal number of parameters and C are determined at levels of 0.001 and 0.01, respectively. This model has a 0.977 accuracy rating. The study's findings support the SVM method's effectiveness in classifying mineralized zones.

2. Methodology

2.1. Martials

Fine DE powder was supplied with a specified BET surface area of 34.10 m^2/g with a 10th, 40 th and 80th size of 1.8, 6.1, and 15.0 μm (Fig. 3). Sulfuric acid (98 wt%), nitric acid, and branched PEI were used for surface modification and acid purification. Sulfuric acid (98 wt%) and branched PEI (MW = 25,000 g/mol) were provided. Purity sodium hydroxide pellets (99.2%), concentrated nitric acid (37%), and sulfuric acid (95%) were applied to make base or acid solutions for pH adjustment. In all tests, deionized water (18.2 MΩ/cm, Labpro water) was utilized. The collection of 40 borehole drill data sets included information on lithology, mineralization, and alteration. 3500 specimens total were gathered for litho-geochemical examination. Inductively Coupled Plasma Atomic Emission Spectroscopy was used to assess the quantity of Copper in lithogeochemical materials (ICP-AES). Fig. 5 shows a schematic presentation of the acid mine drainage treatment process. The correlation matrix between heavy metals ratio and Cu is shown in Table 1.

2.2. Support Vector Machine (SVM)

In order to create nonlinear decision functions for pattern recognition, the SVM technique trains a classifier to do a linear division in a high-dimensional space that isn't linearly connected to the input space.

$$|y - f(x)|_\varepsilon : = \text{m}\ \{0, |y - f(x)| - \varepsilon\} \tag{18}$$

To estimating a linear regression

$$f(x) = (w \cdot x) + b \tag{19}$$

with precision, one minimizes

$$\frac{1}{2}\parallel w\|^2 + C\sum\nolimits_{i=1}^{m} \Big| y - f(x)|_\varepsilon \tag{20}$$

$$L(w, \xi, \xi') = \frac{1}{2}\parallel w\|^2 + C\sum_{i=1}^{N}\left(\xi_i + \xi_i'\right) \tag{21}$$

It should be observed that any mistake less than ε does not need a nonzero ξ_i or ξ_i', and does not enter the objective function, as stated in (20). To identify patterns, generalized kernel-based regression prediction is performed completely analogously. Introducing Lagrange multipliers, the following problem is for $C > 0, \varepsilon > 0$ chosen a priori, " *Maximize*

$$\begin{aligned} L(\alpha, \alpha') = {} & \frac{1}{2}\sum_{i=1}^{N}\sum_{j=1}^{N}(\alpha_i - \alpha_i')x_i^T x_j\left(\alpha_i - \alpha_j'\right) \\ & + \sum_{i=1}^{N}\left((\alpha_i - \alpha_i')y_i - (\alpha_i + \alpha_i')\varepsilon\right) \end{aligned} \tag{22}$$

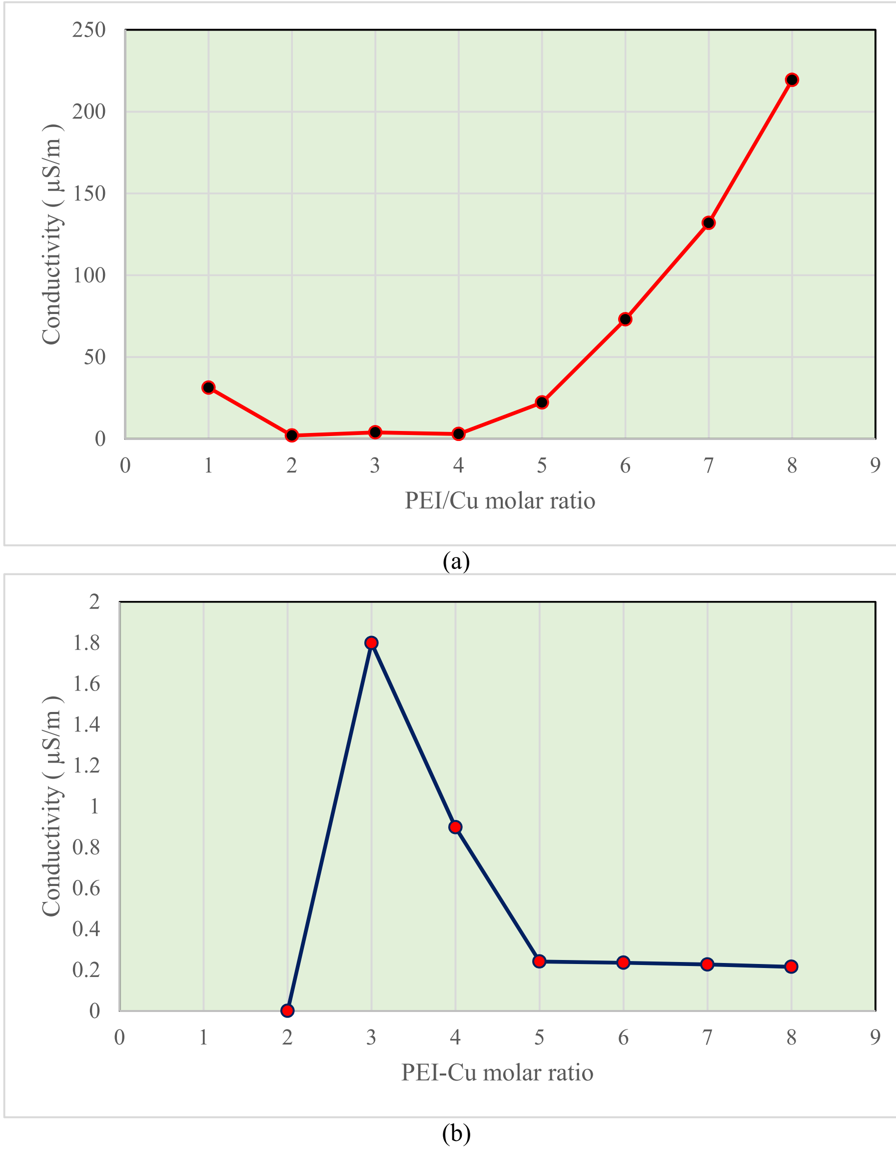

Fig. 6. Ionic strength and high pH facilitated the make of compact and thick layer of self-assembled PEI. The pH was selected in accordance with a prior technique for PEI self-assembly and a measurement that demonstrated that the polymer charge was dramatically reduced when the pH was raised above 9: PEI (M_n ~60,000 and M_w ~750,000) as a function of pH (a). The PEI ratio was 2 mg/mL in 1 mM Nitric acid and pH was adjusted with 1 M Nitric acid and 0.02 M KOH (b).

Subject to $0 \leq (\alpha_i - \alpha_i') \leq C$where, x_i only appears inside an inner product. To get a possibly more accurate providing of the data, the data points might be mapped onto an alternate space, often known as a metric space.

$$x_i x_j \rightarrow \varphi(x_i)\cdot\varphi(x_j) \tag{23}$$

As a result, while data for n-parity or the two spirals issue cannot be divided in the input space by a hyperplane, they may be divided in the feature space by an RBF kernel:

$$k(x_i, x_j) = e^{-\|x_i - x_j\|^2/2\sigma^2} \tag{24}$$

σ = the Gaussian parameter.

Few choices for the kernel could be observed in Table 3. Then, the regression estimation is:

$$y_i = \sum_{i=1}^{N} \sum_{j=1}^{N} (\alpha_i - \alpha_i')\varphi(x_i)^T \varphi(x_j) + b \sum_{i=1}^{N} \sum_{j=1}^{N} (\alpha_i - \alpha_i') K(x_i, x_j) + b \tag{25}$$

$$\text{sgn}\,(x) = \begin{pmatrix} 1 & \text{if } x \succ 0 \\ 0 & \text{if } x = 0 \\ -1 & \text{if } x \prec 0 \end{pmatrix} \tag{26}$$

To calculate $f(x)$, the two factors of decision function w and b could be gained by solving Eq. (27):

$$\text{Minimize } \tau(w) = \frac{1}{2} \parallel w^2 \parallel \tag{27}$$

Subject to

$$y_i((wx_i) + b) \geq 1.i = 1 \ldots l \tag{28}$$

$$L(w, b, \alpha) = \frac{1}{2} \parallel w^2 \parallel - \sum_{i=1}^{l} \alpha_i (y_i((x_i w) + b) - 1 \tag{29}$$

$$\frac{\partial}{\partial b} L(w \cdot b.\alpha) = 0 \cdot \frac{\partial}{\partial w} L(w \cdot b.\alpha) = 0 \tag{30}$$

α_ε = Lagrange multiplier or dual variables

The objective function of the dual defects needs to become high.

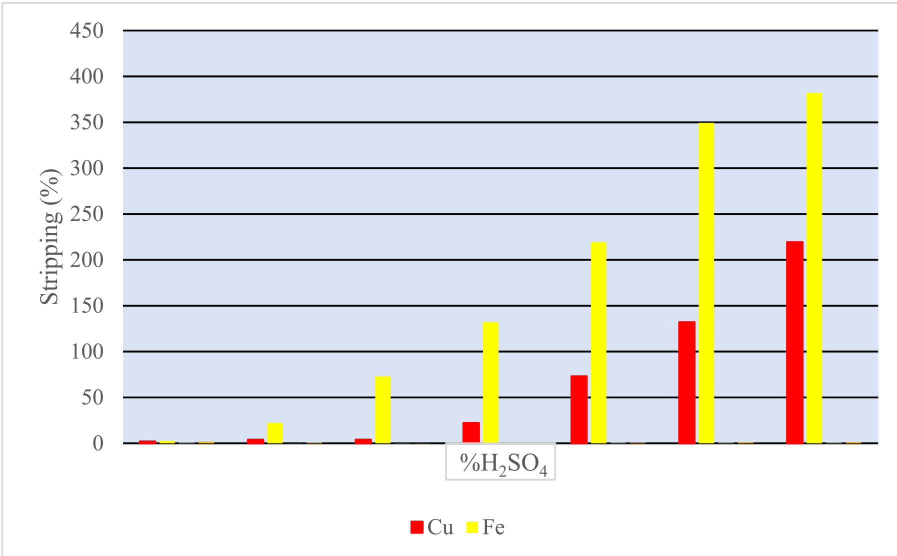

(a)

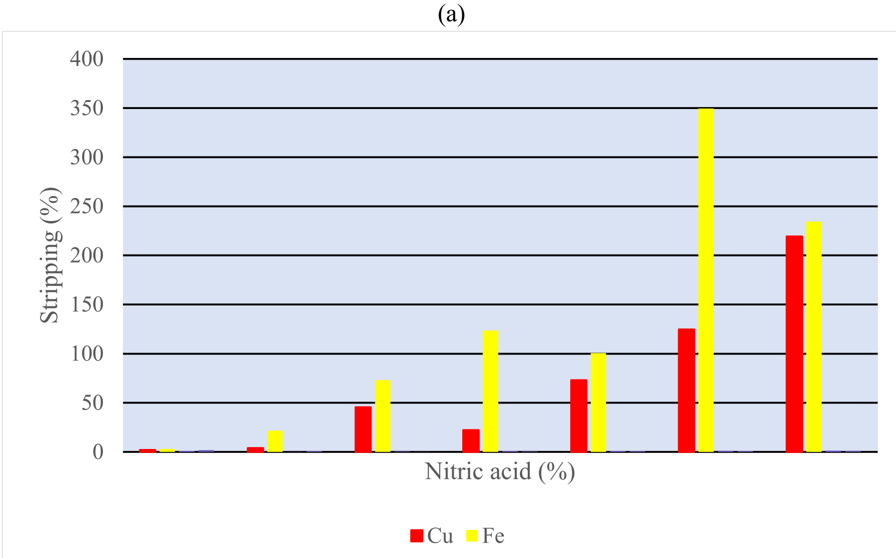

(b)

Fig. 7. The amount of Cu particles of PEI-DE in 10 mL Milli-Q water with a pH value of 4 and 50 mg/L Cu. Added pH was from low to high via Nitric Acid and H_2SO_4 solutions: Fe and copper stripping from loaded 30% (v/v) Acorga M5640 in Shell GTL+2.5% (v/v) octanol (60 min at 25 ± 3 °C) with nitric acid and H_2SO_4 at 0.1 M and with distilled water's control at 1 M and 2 M (a). Further experiment for utilizing the best two acidic solutions at a higher amount of molarities gained the most copper stripping performance of H_2SO_4 acid (b).

$$\text{Maximize} \sum_{j=1}^{l} \alpha_i - \frac{1}{2} \sum_{ij=1}^{l} \alpha_i \alpha_j y_i y_j (x_i, x_j) \tag{31}$$

Subject to

$$\alpha_i \geq 0.\ i = 1 \ldots l. \text{ and } \sum_{i=1}^{l} \alpha_i y_i = 0 \tag{32}$$

3. Result and discussion

As previously mentioned, AMD happens when sulfide minerals are oxidized with oxygen (from the air or dissolved in water) and water (as a vapor or a liquid) to make sulfuric acid. For AMD formation, pyrite's primary reactions are shown below. The first oxidation of pyrite by atmospheric oxygen leads to the production of ferrous (Fe^{2+}) and sulfuric acids as follows:

$$H_2O + FeS_2 + \frac{7}{2O_2} \rightarrow Fe^{2+} + 2H^+ + 2SO_4{}^{2-} \tag{33}$$

$$Fe^{2+} + 1 \Big/ 4O_2 + H^+ \rightarrow 1/2H_2O + Fe^{3+} \tag{34}$$

Oxygen may cause the ferrous iron to undergo further oxidation, causing ferric hydroxide to precipitate and releasing more acid into the atmosphere:

$$Fe^{2+} + 5 \Big/ 2H_2O + 1 \Big/ 4O_2 \rightarrow 2H^+ + Fe(OH)_3 \tag{35}$$

The pH of the solution is reduced while acid production is raised that lead in extra oxidation of pyrite by Fe^{3+} which leads in more acid production:

$$FeS_2 + 14Fe^{3+} + 8H_2O \rightarrow 15Fe^{2+} + 2SO_4^{2-} + 16H^+ \tag{36}$$

The formation ratio depends on a few factors as solution type, type of sulfide and non-sulfide minerals present, type and presence of activating micro-organisms, nutrients, water temperature, the availability of oxygen, and particle size of the rock (Evangelou, 1998). Other common metals, such as zinc, lead, aluminum, and copper, exist since they are found in pyrite-containing rocks. Fig. 8 shows Cu unloading and loading behavior while repetitive cycles include no apparent and it is reduced in the surface modified DE's Cu loading potential at pH 4 (from 500 mg Cu/dm^3 solution) and the efficiency of unloading at pH value of 1 (into pure solution). Also, there are other metal sulfides that could lead in releasing of metal ions into solution (Younger et al., 2002):

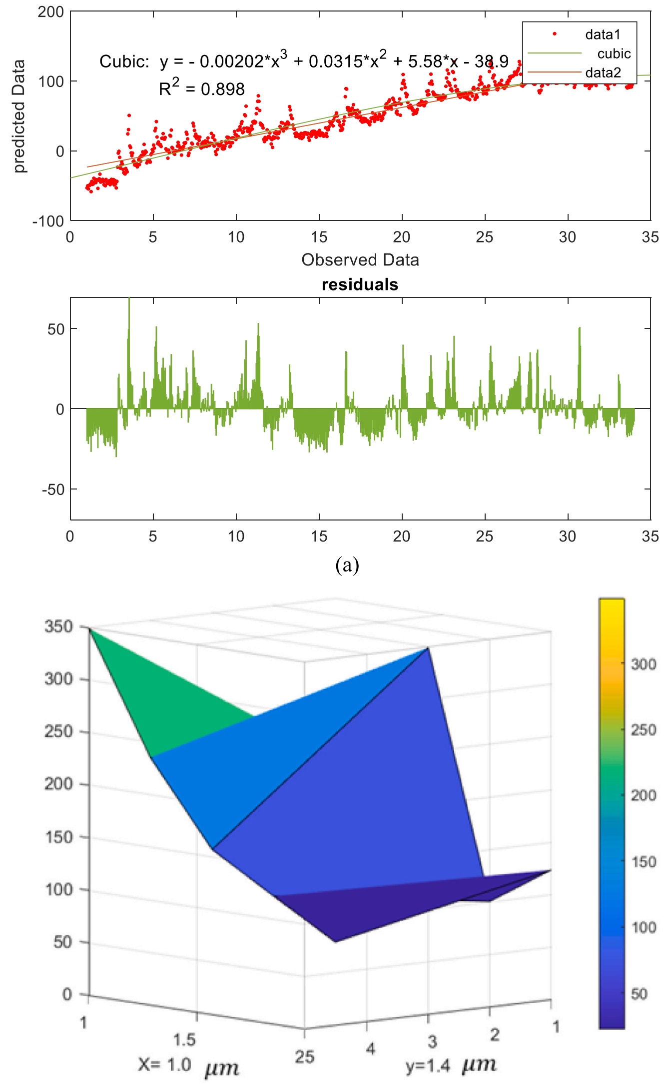

(b)

Fig. 8. Cu unloading/loading behavior while repetitive cycles include no apparent and it is reduced in the surface modified DE's Cu loading potential at pH 4 (from 500 mg Cu/dm^3 solution) and the effeciency of unloading at pH value of 1 (into pure solution).

$$\text{Sphalerite}: \ 2O_2(aq) + ZnS(s) \rightarrow SO_4{}^{2-}(aq) + Zn^{2+}(aq) \quad (37$$

$$\text{Galena}: \ 2O_2(aq) + PbS(s) \rightarrow SO_4{}^{2-}(aq) + Pb^{2+}(aq) \quad (38)$$

$$\text{Millerite}: \ 2O_2(aq) + NiS(s) \rightarrow SO_4{}^{2-}(aq) + Ni^{2+}(aq) \quad (39)$$

$$\text{Chalcopyrite}: \ 4O_2(aq) + CuFeS_2(s) \rightarrow Fe^{2+}(aq) + Cu^{2+}(aq) + SO_4{}^{2-}(aq) \quad (40)$$

It is generally known that proteins and polysaccharides quickly build up on surfaces submerged in saltwater, producing a conditioning layer, and that water also includes considerable quantities of dissolved organic carbon (DOC). Therefore, a differing amount will form on the PEI coatings over time and may have an impact on how much copper is absorbed (Lindén et al., 2016). In a work by Shane et al. a mild acidic cation resin was used (Shane et al., 2021). Cu contents in the treated water were measured by spectrophotometric means using sodium diethyldithiocarbamate. Results indicated that more flow rates are done in less period after that the Cu ratio in the treated water reaches 1 mg/L. The findings of this test showed that ion exchange resins could effectively treat acid mine drainage, but it is also crucial to make proper operating conditions.

Three factors made it crucial to determine how metal binding and precipitation changed with pH using PEI-DE: 1) Because measuring the amount of metal bound to the particles required distinguishing between dissolved and solid material, it was necessary to attribute changes in dissolved metal content to either binding or precipitation to the PEI-DE at various pH levels, 2) It's crucial to comprehend how well the particles remove copper at various pH levels because particles of surface-modified DE (PEI-DE) have a strong pH dependence, 3) Pure copper solutions can be made by selectively extracting copper and then eluting it with reducing the pH in the method of copper extraction (Larsson et al., 2018). Nonetheless, precipitated metal hydroxides created while the extraction process of Cu would also dissolve in an environment with low pH, producing mixed metal solutions. When PEI-DE particles were present, the copper ratio began to drop as early as pH 2, only 8% of the copper was still in solution at pH 3, and just 1% of the copper was still in solution at pH 4 and 5 $\leq$ 1%. The remaining amount of iron in solution get reduced substantially from pH of 3 in the existence of the particles of PEI -DE, and with pH levels of 4 and 5 the remaining fraction was 14.2% and 2.3%, respectively. Table 4 show the AMD properties. Table 2 shows SVM's optimum value and training range parameters. Table 3 shows R^2 and RMSE of SVM in train and test data. Table 4 shows composition of Acid Mine Drainage. Fig. 6 shows Ionic strength and high pH facilitated the make of compact and thick layer of self-assembled PEI. PH was selected in accordance with a prior technique for PEI self-assembly and measuring that the polymer charge was dramatically reduced when the pH was raised above 9: PEI (M_n ~60,000 and M_w ~750,000) as a function of pH. The PEI ratio was 2 mg/mL in 1 mM Nitric acid and pH was adjusted with 1 M Nitric acid and 0.02 M KOH.

4. Conclusion

The amount of PEI in solution had no effect on the coating's thickness. With the PEI coating on diatomaceous earth particles as the carrier material, very effective removal of copper from water was shown to be practical, showing promise for extraction of copper from polluted water. It has been shown that PE-DE particles may be used to recover copper more effectively using both model and actual acid mine drainage (AMD) solutions. The SVM is a novel machine learning methodology with a number of notable characteristics, such as the kernel requirement and the nature of the optimization problem. Using the SVM algorithm to forecast Cu affected by AMD has been provided in this work. According to the SVM results, all of the data falls between $0 \leqslant H \leqslant 0.055$ and $-1 \leqslant R \leqslant 1$ with correlation values greater than 0.99. Compared to the requirements of the model, these ranges provide substantially superior confidence bounds. The data demonstrate how precise and trustworthy the constructed model is, with deviation's average absolute relative percentage of 4.8% and coefficients of correlation that are nearly united. Despite the fact that the approach used data-driven models, the analysis time was much shorter and the accuracy was greater. Additionally, the model can accurately forecast the equilibrium adsorption trend as a function of the initial concentration of metal at various PHs. Even though acidification decreased the ability of Cu^{2+} and PEI to form complexes, which made it easier for the metal to get out, PEI still illustrated a strong level of chelation with Cu^{2+} at a ratio of 4 M. Additionally, when the optimum PEI concentrations were used, removal of Cu^{2+} above 99.1% was accomplished. With the exception of copper, all metal ratios were found to be very low after metal binding by particles of PEI-DE at pH value of 4. The level of copper, however, was lowered to 1 mg/L. Future studies will focus on more optimizing the technique for large-scale uses and applying the material to produce pure Cu solutions from complicated solutions as AMD. This will need the development of a mechanism for controlling particle size so that sufficient flow may be attained in columns, as well as enhancing the material's capacity by decreasing the proportion of non-PEI-DE in the particles.

Funding

China Scholarship Council (CSC):Innovative Talents Training Project for Ecological Protection and Quality Development of the Yellow River Bone Region in Henan Province in 2021 (NO.202108410349).

Authorship statement

All persons who meet authorship criteria are listed as authors, and all authors certify that they have participated sufficiently in the work to take public responsibility for the content, including participation in the concept, design, analysis, writing, or revision of the manuscript. Furthermore, each author certifies that this material or similar material has not been and will not be submitted to or published in any other publication before its appearance in the Chemosphere Journal.

Authorship contributions

Mingfei Ji: Methodology, Validation; Supervision, Project administration; Resources, Bailian Li: Data curation. Writing - review & editing; Conceptualization, Writing-review and editing, Ali Majdi: Data curation. Writing - review & editing; Conceptualization, Tamim Alkhalifah: Data curation. Writing - review & editing; Conceptualization, Software; Conceptualization, Writing-review and editing, Fahad Alturise: Data curation. Writing - review & editing; Conceptualization, H. Elhosiny Ali: Data curation. Writing - review & editing; Conceptualization, Software; Conceptualization, Writing-review and editing.

Declaration of competing interest

The authors declare that they have no known competing financial interests or personal relationships that could have appeared to influence the work reported in this paper.

Data availability

Data will be made available on request.

Acknowledgments

The authors extend their appreciation to the Research Center for Advanced Materials Science (RCAMS), King Khalid University, Saudi Arabia, for funding this work under grant number R.G.P.2/120/43. This work was supported by Al-Mustaqbal University College Grant number = MUC -M-0222.

References

Abbaszadeh, M., Hezarkhani, A., Soltani-Mohammadi, S., 2013. An SVM-based machine learning method for the separation of alteration zones in Sungun porphyry copper deposit. Geochemistry 73 (4), 545–554.
Abd Majid, M.Z., et al., 2015a. Controlling stormwater runoff pollution best practices of green highway developments. J. Environ. Treat. Techniq. 4 (4), 170–172.
Abd Majid, M.Z., et al., 2015b. Green highway development features to control stormwater runoff pollution. J. Environ. Treat. Techniq. 4 (4), 173–175.
Abdullah, A.H., et al., 2022. A comprehensive review of nanoparticles in water-based drilling fluids on wellbore stability. Chemosphere 136274.
Adler, R., Rascher, J., 2007. A Strategy for the Management of Acid Mine Drainage from Gold Mines in Gauteng. Contract Report for Thutuka (Pty) Ltd. Submitted by the Water Resource Governance Systems Research Group, CSIR: Pretoria. Report No. CSIR/NRE/PW/ER/2007/0053/C.
Ahmad, A., Buang, A., Bhat, A., 2016. Renewable and sustainable bioenergy production from microalgal co-cultivation with palm oil mill effluent (POME): a review. Renew. Sustain. Energy Rev. 65, 214–234.
Aivalioti, M., et al., 2012. Adsorption of BTEX, MTBE and TAME on natural and modified diatomite. J. Hazard Mater. 117–127, 207-208.
Akinwekomi, V., et al., 2016. Integrated acid mine drainage treatment using Mg(OH)2 or Mg(HCO3)2 and Ca(OH)2: implications for separate removal of metals and sulphate. Int. J. Miner. Process. 155, 83–90.
Al-Dailami, A., et al., 2022. Sustainable solid waste management in Yemen: environmental, social aspects, and challenges. Biomass Convers. Biorefinery 1–27.
Alothman, Z.A., Apblett, A.W., 2010. Metal ion adsorption using polyamine-functionalized mesoporous materials prepared from bromopropyl-functionalized mesoporous silica. J. Hazard Mater. 182 (1), 581–590.
Anita, M.R., et al., 2014. Effect of temperature on theperformance of porous membrane activated sludge reactor (PMASR) treating synthetic wastewater. Research journal of pharmaceutical. Biol. Chem. Sci. 5 (1), 84–100.
Arabi-Nowdeh, S., et al., 2021. Multi-criteria optimal design of hybrid clean energy system with battery storage considering off-and on-grid application. J. Clean. Prod. 290, 125808.
Arabnejad Khanouki, M., Ramli Sulong, N., Shariati, M., 2010a. Investigation of seismic behaviour of composite structures with concrete filled square steel tubular (CFSST) column by push-over and time-history analyses. In: Proceedings of the 4th International Conference on Steel Composite Structures.
Arabnejad Khanouki, M.M., Ramli Sulong, N.H., Shariati, M., 2010b. Investigation of seismic behaviour of composite structures with concrete filled square steel tubular (CFSST) column by push-over and time-history analyses. In: Proceedings of the 4th International Conference on Steel & Composite Structures.
Arora, S., Vadhera, R., Chugh, B., 2021. A decision-making system for Corona prognosis using fuzzy inference system. J. Fuzzy Ext. Appl. 2 (4), 344–354.
Ashokkumar, V., et al., 2019. Cultivation of microalgae Chlorella sp. in municipal sewage for biofuel production and utilization of biochar derived from residue for the conversion of hematite iron ore (Fe2O3) to iron (Fe)–Integrated algal biorefinery. Energy 189, 116128.
Awual, M.R., et al., 2013. Rapid recognition and recovery of gold(III) with functional ligand immobilized novel mesoporous adsorbent. Microchem. J. 110, 591–598.
Azizan, N.A.Z., et al., 2022a. The effects of caffeine, gliclazide, and prazosin on the performance and microbial diversity in an up-flow anaerobic sludge blanket (UASB) reactor. Biomass Bioenergy 163, 106511.
Azizan, N.A.Z., et al., 2022b. The selectivity of electron acceptors for the removal of caffeine, gliclazide, and prazosin in an up-flow anaerobic sludge blanket (UASB) reactor. Chemosphere 303, 134828.
Babaee Khobdeh, S., Yamaghani, M.R., Khodaparast Sareshkeh, S., 2021. Clustering of basketball players using self-organizing map neural networks. J. Appl. Res. Ind. Eng> 8 (4), 412–428.
Balaraman, P., et al., 2020. Phyco-synthesis of silver nanoparticles mediated from marine algae Sargassum myriocystum and its potential biological and environmental applications. Waste Biomass Valorization 11 (10), 5255–5271.
Banfield, J., 1997. Geomicrobiology: interactions between microbes and minerals. Rev. Mineral. 35, 448.
Banfield, J.F., Nealson, K.H., 2018. Walter de Gruyter GmbH & Co KG. Geomicrobiology: Interactions between microbes and minerals 35.
Bardi, U., 2010. Extracting minerals from seawater: an energy analysis. Sustainability 2 (4), 980–992.
Bariana, M., et al., 2013. Tuning drug loading and release properties of diatom silica microparticles by surface modifications. Int. J. Pharm. 443 (1), 230–241.
Beatty, S.T., et al., 1999. Comparison of novel and patented silica-polyamine composite materials as aqueous heavy metal ion recovery materials. Separ. Sci. Technol. 34 (14), 2723–2739.
Black, A., Craw, D., 2001. Arsenic, copper and zinc occurrence at the Wangaloa coal mine, southeast Otago, New Zealand. Int. J. Coal Geol. 45 (2), 181–193.
Bridge, Johnson D., Hallberg, Kevin B., 2005. Acid Mine Drainage Remediation, School of Biological Sciences, vol. 338. University of Wales, Bangor, UK, pp. 3–14.
Bulut, U., Özceylan, E., 2021. Application of the fuzzy inference system to evaluate the quality of air textured warp yarn. In: International Conference on Intelligent and Fuzzy Systems. Springer.
Bwapwa, J.K., Jaiyeola, A.T., Chetty, R., 2017. Bioremediation of acid mine drainage using algae strains: a review. S. Afr. J. Chem. Eng. 24, 62–70.
Chahnasir, E.S., et al., 2018. Application of support vector machine with firefly algorithm for investigation of the factors affecting the shear strength of angle shear connectors. Smart Struct. Syst. 22 (4), 413–424.
Chanda, M., Pillay, S.A., 2005. A novel fibre-coated sorbent for rapid removal of heavy metals from wastewater. Sorption of Zinc (II) from dilute aqueous solutions in the presence of high concentrations of common salts.
Cheah, W.Y., et al., 2018. Microalgae cultivation in palm oil mill effluent (POME) for lipid production and pollutants removal. Energy Convers. Manag. 174, 430–438.
Chelliapan, S., et al., 2020. Anaerobic Treatment of Municipal Solid Waste Landfill Leachate, in Bioreactors. Elsevier, pp. 175–193.
Chouyyok, W., et al., 2010. Selective removal of copper (II) from natural waters by nanoporous sorbents functionalized with chelating diamines. Environ. Sci. Technol. 44 (16), 6390–6395.
Deng, S., Ting, Y.P., 2005a. Polyethylenimine-modified fungal biomass as a high-capacity biosorbent for Cr (VI) anions: sorption capacity and uptake mechanisms. Environ. Sci. Technol. 39 (21), 8490–8496.
Deng, S., Ting, Y.-P., 2005b. Characterization of PEI-modified biomass and biosorption of Cu(II), Pb(II) and Ni(II). Water Res. 39 (10), 2167–2177.
Duda, R.O., Hart, P.E., 2006. John wiley & sons. Pattern classif.
Duda, R.O., Hart, P.E., Stork, D.G., 1973. Pattern Classif. Scene Anal. 3 (Wiley New York).
Duffus, J.H., 2002. *A meaningless term?(IUPAC Technical Report)*. Pure and applied chemistry. Heavy metals 74 (5), 793–807.
Duru, P.E., et al., 2001. Adsorption of heavy-metal ions on poly (ethylene imine)-immobilized poly (methyl methacrylate) microspheres. J. Appl. Polym. Sci. 81 (1), 197–205.
El-Khoribi, R.A., 2008. Support vector machine training of HMT models for land cover image classification. ICGST-GVIP 8 (4), 7–11.

Esfahan, Z.M., Izhar, S., Halim, M., 2020. Synthesis and swelling kinetic study of BSA-based hydrogel composite by subcritical water technology. J. Environ. Treat. Techniq. 8 (2), 756–761.
Evangelou, V., 1998. *Pyrite Chemistry: the Key for Abatement of Acid Mine Drainage*, in *Acidic Mining Lakes*. Springer, pp. 197–222.
Eyo, I.J., et al., 2022. Hybrid intelligent parameter tuning approach for COVID-19 time series modeling and prediction. J. Fuzzy Ext. Appl. 3 (1), 64–80.
Foong, L.K., et al., 2021. Efficient metaheuristic-retrofitted techniques for concrete slump simulation. Smart Structures and Systems. Int. J. 27 (5), 745–759.
Gaikwad, R.W., Gupta, D.V., 2008. Review on removal of heavy metals from acid mine drainage. Appl. Ecol. Environ. Res. 6 (3), 81–98.
Gao, B., et al., 2005. Studies on the surface modification of diatomite with polyethyleneimine and trapping effect of the modified diatomite for phenol. Appl. Surf. Sci. 250 (1), 273–279.
Ge, D., Yuan, H., Xiao, J., Zhu, N., 2019. Insight into the enhanced sludge dewaterability by tannic acid conditioning and pH regulation. The Science of the total environment 679, 298–306. https://doi.org/10.1016/j.scitotenv.2019.05.060.
Guan, Q., Zeng, G., Song, J., Liu, C., Wang, Z., Wu, S., 2021. Ultrasonic power combined with seed materials for recovery of phosphorus from swine wastewater via struvite crystallization process. Journal of environmental management 293, 112961. https://doi.org/10.1016/j.jenvman.2021.112961.
Hosseini, M., et al., 2019. Preparation, and structural of new NiS-SiO2 and Cr2S3-TiO2 nano-catalyst: photocatalytic and antimicrobial studies. J. Photochem. Photobiol. B Biol. 194, 128–134.
Hosur Shivaramaiah, N.K., et al., 2022. Geometrically nonlinear behavior of two-directional functionally graded porous plates with four different materials. Proc. IME C J. Mech. Eng. Sci., 09544062221111038
Hubicki, Z., Kołodyńska, D., 2012. Selective removal of heavy metal ions from waters and waste waters using ion exchange methods. Ion Exchange Technol. 7, 193–240.
Iiyama, M., et al., 2004. Adsorption of divalent transition metal ions with a chelating agent on octadecyl silica gel. Anal. Sci. 20 (10), 1463–1464.
Ilmasari, D., et al., 2022. A Review of the biological Treatment of leachate: available Technologies and future Requirements for the circular economy implementation. Biochem. Eng. J. 108605.
Jamal, A., et al., 2015. Heavy metals from acid mine drainage in coal mines-a case study. Eur. J. Adv. Eng. Technol. 2 (8), 16–20.
Jennings, S.R., Blicker, P.S., Neuman, D.R., 2008. Reclamation research group. Acid mine drainage and effects on fish health and ecology: Rev.
John, H.D., 2002. Heavy metals'a meaningless term. Pure Appl. Chem. 74 (5), 793.
Johnson, D.B., Hallberg, K.B., 2005. Acid mine drainage remediation options: a review. Sci. Total Environ. 338 (1), 3–14.
Kagambega, N., et al., 2014. Acid mine drainage and heavy metals contamination of surface water and soil in southwest Burkina Faso-West Africa. Int. J. Multidiscip. Acad. Res. 2 (3), 9–19.
Kamyab, H., et al., 2014a. Microalgae Chlorella vulgaris as promising agent for treating palm oil mill effluent (POME). Energy Proc. 75, 2400–2408.
Kamyab, H., et al., 2014b. Micro-macro algal mixture as a promising agent for treating POME discharge and its potential use as animal feed stock enhancer. J. Teknologi 68 (5).
Kamyab, H., et al., 2014c. Effects of nitrogen source on enhancing growth conditions of green algae to produce higher lipid. Desalination Water Treat. 52 (19–21), 3579–3584.
Kamyab, H., et al., 2016a. Isolation and screening of microalgae from agro-industrial wastewater (POME) for biomass and biodiesel sources. Desalination Water Treat. 57 (60), 29118–29125.
Kamyab, H., et al., 2016b. Optimum lipid production using agro-industrial wastewater treated microalgae as biofuel substrate. Clean Technol. Environ. Policy 18 (8), 2513–2523.
Kamyab, H., et al., 2016c. Chlorella pyrenoidosa mediated lipid production using Malaysian agricultural wastewater: effects of photon and carbon. Waste Biomass Valorization 7 (4), 779–788.
Kamyab, H., et al., 2022a. A review on carbon-based molecularly-imprinted polymers (CBMIP) for detection of hazardous pollutants in aqueous solutions. Chemosphere 136471.
Kamyab, H., et al., 2022b. Electrochemical oxidation of palm oil mill effluent using platinum as anode: optimization using response surface methodology. Environ. Res. 214, 113993.
Karimi, H., et al., 2016. An analytical approach to calculate the charge density of biofunctionalized graphene layer enhanced by artificial neural networks. Plasmonics 11 (1), 95–102.
Khoshnava, S.M., et al., 2020. Green efforts to link the economy and infrastructure strategies in the context of sustainable development. Energy 193, 116759.
Kleinmann, R., 1985. Treat. Acid Mine water by Wetlands.
Kokila, R., et al., 2021. A GIS-based tool for the analysis of the distribution and abundance of Chilo sacchariphagus indicus under the influence of biotic and abiotic factors. Environ. Technol. Innovat. 21, 101357.
Krishnan, S., et al., 2021. Application of bioelectrochemical systems in wastewater treatment and hydrogen production. In: Delivering Low-Carbon Biofuels with Bioproduct Recovery. Elsevier, pp. 31–44.
Krishnan, S., et al., 2022. Fouling characteristics and cleaning approach of ultrafiltration membrane during xylose reductase separation. Bioproc. Biosyst. Eng. 1–12.
Larsson, M., et al., 2018. Copper removal from acid mine drainage-polluted water using glutaraldehyde-polyethyleneimine modified diatomaceous earth particles. Heliyon 4 (2), e00520.
Lin, H., et al., 2022. Technologies for removing heavy metal from contaminated soils on farmland: a review. Chemosphere 135457.
Lindén, J.B., et al., 2015. Polyethyleneimine for copper absorption II: kinetics, selectivity and efficiency from seawater. RSC Adv. 5 (64), 51883–51890.
Lindén, J.B., et al., 2016. Glutaraldehyde-crosslinking for improved copper absorption selectivity and chemical stability of polyethyleneimine coatings. J. Appl. Polym. Sci. 133 (37).
Liu, W., Huang, F., Liao, Y., Zhang, J., Ren, G., Zhuang, Z., Wang, C., 2008. Treatment of CrVI-containing Mg(OH)2 nanowaste. Angew. Chem. (Int. Ed.) 47 (30), 5619–5622. https://doi.org/10.1002/anie.200800172.
Liu, Y., Zhang, Z., Liu, X., Wang, L., Xia, X., 2021. Efficient image segmentation based on deep learning for mineral image classification. Adv. Powder Technol. 32 (10), 3885–3903. https://doi.org/10.1016/j.apt.2021.08.038.
Lottermoser, B., 2010. Mine Wastes: Characterization, Treatment and Environmental Impacts, pp. 1–400.
Maketon, W.K., Ogden, K.L., 2008. Treatment of copper from Cu CMP waste streams using polyethyleneimine. IEEE Trans. Semicond. Manuf. 21 (3), 481–485.
Marynirmala, J., Sivakumar, D., 2021. Pythagorean fuzzy weak bi-ideals of Γ-near ring. J. Fuzzy Ext. Appl. 2 (3), 297–320.
Maslahati Roudi, A., et al., 2018. Prediction and optimization of the fenton process for the treatment of landfill leachate using an artificial neural network. Water 10 (5), 595.
McCarthy, T.S., 2011. The impact of acid mine drainage in South Africa. South Afr. J. Sci. 107 (5), 1–7.
Michael, M., et al., 2022. The content of heavy metals in cigarettes and the impact of their leachates on the aquatic ecosystem. Sustainability 14 (8), 4752.
Milovančević, M., et al., 2019. UML diagrams for dynamical monitoring of rail vehicles. Phys. Stat. Mech. Appl. 531, 121169.
Mohammadhassani, M., et al., 2014. An evolutionary fuzzy modelling approach and comparison of different methods for shear strength prediction of high-strength concrete beams without stirrups. Smart Struct. Syst. 14 (5), 785–809.
Nilashi, M., et al., 2019. Measuring sustainability through ecological sustainability and human sustainability: a machine learning approach. J. Clean. Prod. 240, 118162.
Nor, F.H.M., et al., 2022. Role of extremophilic Bacillus cereus KH1 and its lipopeptide in treatment of organic pollutant in wastewater. Bioproc. Biosyst. Eng. 1–11.
Nordstrom, D.K., Southam, G., 1997. Geomicrobiol. Sulf. Miner. Oxid.
Offeddu, F.G., et al., 2015. Processes affecting the efficiency of limestone in passive treatments for AMD: column experiments. J. Environ. Chem. Eng. 3 (1), 304–316.
Oryani, B., et al., 2022. Assessing the financial resource curse hypothesis in Iran: the novel dynamic ARDL approach. Resour. Pol. 78, 102899.
Othman, N., et al., 2021. A Design Framework for an Integrated End-Of-Life Vehicle Waste Management System in Malaysia, in Soft Computing Techniques in Solid Waste and Wastewater Management. Elsevier, pp. 305–319.
Pan, D., Chen, H., 2021. Border pollution reduction in China: The role of livestock environmental regulations. China economic review 69, 101681. https://doi.org/10.1016/j.chieco.2021.101681.
Pang, Y., et al., 2011. PEI-grafted magnetic porous powder for highly effective adsorption of heavy metal ions. Desalination 281, 278–284.
Pierson-Wickmann, A.-C., et al., 2011. Development of a combined isotopic and mass-balance approach to determine dissolved organic carbon sources in eutrophic reservoirs. Chemosphere 83 (3), 356–366.
Prasad, S., et al., 2020. Screening and evaluation of cellulytic fungal strains for saccharification and bioethanol production from rice residue. Energy 190, 116422.
Putri, E.V., et al., 2011. Investigation of microalgae for high lipid content using palm oil mill effluent (Pome) as carbon source. In: International Conference on Environment and Industrial Innovation. IPCBEE. Citeseer.
Qureshi, F., et al., 2022a. Latest eco-friendly avenues on hydrogen production towards a circular bioeconomy: currents challenges, innovative insights, and future perspectives. Renew. Sustain. Energy Rev. 168, 112916.
Qureshi, F., et al., 2022b. Current trends in hydrogen production, storage and applications in India: a review. Sustain. Energy Technol. Assessments 53, 102677.
Rezania, S., et al., 2017. Review on pretreatment methods and ethanol production from cellulosic water hyacinth. Bioresources 12 (1), 2108–2124.
Rezania, S., et al., 2018. Ethanol production from water hyacinth (Eichhornia crassipes) using various types of enhancers based on the consumable sugars. Waste Biomass Valorization 9 (6), 939–946.
Rezania, S., et al., 2019. Effect of various pretreatment methods on sugar and ethanol production from cellulosic water hyacinth. Bioresources 14 (1), 592–606.
Rezania, S., et al., 2022. Lanthanum doped magnetic polyaniline for removal of phosphate ions from water. Chemosphere 307, 135809.
Richards, J., 2003. Tectono-magmatic precursors for porphyry Cu-(Mo-Au) deposit formation. Econ. Geol. 98 (8), 1515–1533.
Roudi, M., 2014. Biodiesel production from microalgae-Chlorella sorokoniana. Australian J. Basic Appl. Sci. 8 (3), 140–145.
Safari, M., Maghsoudi, A., Pour, A.B., 2018. Application of Landsat-8 and ASTER satellite remote sensing data for porphyry copper exploration: a case study from Shahr-e-Babak, Kerman, south of Iran. Geocarto Int. 33 (11), 1186–1201.
Schiff, K., 2004. *d. diehl and a. Valkirs.* Mar. Pollut. Bull. (Arch. Am. Art) 48, 371.
Schwochau, K., 1984. Extraction of Metals from Sea Water, in Inorganic Chemistry. Springer, pp. 91–133.
Selvama, S.B., et al., 2019. Landfill leachate treatment by an anaerobic process enhanced with recyclable uniform beads (RUB) of seaweed species of Gracilaria. Desalination Water Treat. 143, 208–216.
Setia, R., et al., 2021. Phytoavailability and human risk assessment of heavy metals in soils and food crops around Sutlej river, India. Chemosphere 263, 128321.
Shabalala, A.N., et al., 2017. Pervious concrete reactive barrier for removal of heavy metals from acid mine drainage – column study. J. Hazard Mater. 323, 641–653.

Shah, S., et al., 2016a. Behavior of steel pallet rack beam-to-column connections at elevated temperatures. Thin-Walled Struct. 106, 471–483.
Shah, S., et al., 2016b. Behavior of industrial steel rack connections. Mech. Syst. Signal Process. 70, 725–740.
Shane, A., et al., 2021. Removal of Copper from Acid Mine Drainage (AMD) or Acid Rock Drainage (ARD).
Shariati, M., et al., 2011a. Experimental and numerical investigations of channel shear connectors in high strength concrete. In: Proceedings of the 2011 World Congress on Advances in Structural Engineering and Mechanics (ASEM'11+), Seoul, South Korea.
Shariati, M., et al., 2011b. Experimental and numerical investigations of channel shear connectors in high strength concrete. In: Proceedings of the 2011 World Congress on Advances in Structural Engineering and Mechanics (ASEM'11+).
Shariati, M., et al., 2012a. Fatigue energy dissipation and failure analysis of channel shear connector embedded in the lightweight aggregate concrete in composite bridge girders. In: Proceedings of the 5th International Conference on Engineering Failure Analysis. ICEFA.
Shariati, M., et al., 2012b. Fatigue energy dissipation and failure analysis of channel shear connector embedded in the lightweight aggregate concrete in composite bridge girders. In: Fifth International Conference on Engineering Failure Analysis 1-4 July 2012, Hilton Hotel, the Hague, The Netherlands.
Shariati, M., et al., 2019a. Application of waste tire rubber aggregate in porous concrete. Smart Structures and Systems. Int. J. 24 (4), 553–566.
Shariati, M., et al., 2019b. Application of a hybrid artificial neural network-particle swarm optimization (ANN-PSO) model in behavior prediction of channel shear connectors embedded in normal and high-strength concrete. Appl. Sci. 9 (24), 5534.
Shariati, M., et al., 2020a. Prediction of concrete strength in presence of furnace slag and fly ash using Hybrid ANN-GA (Artificial Neural Network-Genetic Algorithm). Smart Structures and Systems. Int. J. 25 (2), 183–195.
Shariati, M., et al., 2020b. Monotonic behavior of C and L shaped angle shear connectors within steel-concrete composite beams: an experimental investigation. Steel Compos. Struct. 35 (2), 237–247.
Shariati, M., et al., 2020c. Evaluation of seismic performance factors for tension-only braced frames. Steel Compos. Struct. 35 (4), 599–609.
Shariati, M., et al., 2020d. A novel hybrid extreme learning machine–grey wolf optimizer (ELM-GWO) model to predict compressive strength of concrete with partial replacements for cement. Eng. Comput. 1–23.
Shariati, M., et al., 2020e. Numerical study on the axial compressive behavior of built-up CFT columns considering different welding lines. Steel Compos. Struct. 34 (3), 377–391.
Shariati, M., et al., 2021a. Alkali-activated slag (AAS) paste: Correlation between durability and microstructural characteristics. Construct. Build. Mater. 267, 120886.
Shariati, M., et al., 2021b. Assessment of longstanding effects of fly ash and silica fume on the compressive strength of concrete using extreme learning machine and artificial neural network. J. Adv. Eng. Comp. 5 (1), 50–74.
Sharma, P., et al., 2022. Hydrogen Sulfide: a new warrior in assisting seed germination during adverse environmental conditions. Plant Growth Regul. 1–20.
Sheoran, A.S., Sheoran, V., 2006. Heavy metal removal mechanism of acid mine drainage in wetlands: a critical review. Miner. Eng. 19 (2), 105–116.
Shi, X., et al., 2020. Ultrasound wave assisted removal of Ceftriaxone sodium in aqueous media with novel nano composite g-C3N4/MWCNT/Bi2WO6 based on CCD-RSM model. Ultrason. Sonochem. 68, 104460.
Shu, L., et al., 2021. Assessment methodology applied to arsenic pollution in lake sediments combining static and dynamic processes. Chemosphere 277, 130260.
Simate, G.S., Ndlovu, S., 2014. Acid mine drainage: challenges and opportunities. J. Environ. Chem. Eng. 2 (3), 1785–1803.
Singh, G., 1987. Mine water quality deterioration due to acid mine drainage. Int. J. Mine water 6 (1), 49–61.
Singh, G., Bhatnagar, M., 1985. Bacterial formation of acid mine drainage, causes and control. J. Sci. Ind. Res. 44 (9), 478–485.
Soltani, M., Kamyab, H., El-Enshasy, H.A., 2013. Molecular weight (Mw) and Monosaccharide composition (MC): Two major factors affecting the therapeutic action of polysaccharides extracted from Cordyceps sinensis. J. Pure Appl. Microbiol. 7 (3), 1601–1613.
Soni, A., Das, P.K., 2022. Development of sand-plastic composites as floor tiles using silica sand and recycled thermoplastics mixture from post-consumer products-A sustainable approach for cleaner production.
Soni, A., et al., 2022. Challenges and opportunities of utilizing municipal solid waste as alternative building materials for sustainable development goals: a review. Sustain. Chem. Pharma. 27, 100706.
Steinmann, L., et al., 1994. Preparation and some properties of a polyethyleneimine-agarose metal adsorbent. Talanta 41 (10), 1707–1713.
Taylor, J., Pape, S., Murphy, N., 2005. A summary of passive and active treatment technologies for acid and metalliferous drainage (AMD). In: Proceedings of the in Fifth Australian Workshop on Acid Mine Drainage.
Teimoori, M., et al., 2021. A multi-objective grey wolf optimization algorithm for aircraft landing problem. J. Appl. Res. Ind. Eng. 8 (4), 386–398.
Vadivelu, B., et al., 2020. Synthesis of silver nanoparticles from fish scale extract of Cyprinus carpio and its decolorization activity of textile dyes. J. Environ. Treat Technol. 8, 870–874.
Vasseghian, Y., et al., 2022. Metal-organic framework-enabled pesticides are an emerging tool for sustainable cleaner production and environmental hazard reduction. J. Clean. Prod. 133966.
Velu, M., et al., 2021. Fabrication of nanocomposites mediated from aluminium nanoparticles/Moringa oleifera gum activated carbon for effective photocatalytic removal of nitrate and phosphate in aqueous solution. J. Clean. Prod. 281, 124553.
Wang, B., Smith, T.R., 2007. Performance of a diatomite-based sorbent in removing mercury from aqueous and oil matrices. J. Environ. Eng. Sci. 6 (5), 469–476.
Yadav, V.K., et al., 2022. A novel approach for the synthesis of vaterite and calcite from incense sticks ash waste and their potential for remediation of dyes from aqueous solution. Sustain. Chem. Pharma. 29, 100756.
Yan, B., et al., 2019. Geometrically enabled soft electroactuators via laser cutting. Adv. Eng. Mater. 21 (11), 1900664.
Yang, J., et al., 2022. Heavy metal pollution in agricultural soils of a typical volcanic area: risk assessment and source appointment. Chemosphere 135340.
Yavari, S., et al., 2022. Bio-efficacy of imidazolinones in weed control in a tropical paddy soil amended with optimized agrowaste-derived biochars. Chemosphere 134957.
Yazdani, M., et al., 2021. Improving construction and demolition waste collection service in an urban area using a simheuristic approach: a case study in Sydney, Australia. J. Clean. Prod. 280, 124138.
Younger, P., Banwart, S., Hedin, R., 2002. Mine Water: Hydrology, Pollution, Remediation. KluwerAcademic Publishers, Dordrecht, Netherlands.
Yu, Y., Addai-Mensah, J., Losic, D., 2012. Functionalized diatom silica microparticles for removal of mercury ions. Sci. Technol. Adv. Mater. 13 (1), 015008.
Zain, S.M., et al., 2022. Analysis of Serum Circulating MicroRNAs Level in Malaysian Patients with Gestational Diabetes Mellitus.
Zainah, T.A.S.M.I., Shahaboddin, S.M.S.M.S., 1801. Potential of soft computing approach for evaluating the factors affecting the capacity of steel–concrete composite beam. J. Intell. Manuf. 29 (8), 1793.
Zhang, M., Wang, H., Han, X., 2016. Preparation of metal-resistant immobilized sulfate reducing bacteria beads for acid mine drainage treatment. Chemosphere 154, 215–223.
Zhao, Y., Foong, L.K., 2022. Predicting electrical power output of combined cycle power plants using a novel artificial neural network optimized by electrostatic discharge algorithm. Measurement 111405.
Zhao, Y., Wang, Z., 2022. Subset simulation with adaptable intermediate failure probability for robust reliability analysis: an unsupervised learning-based approach. Struct. Multidiscip. Optim. 65 (6), 1–22.
Zhao, Y., et al., 2020a. Deterministic snap-through buckling and energy trapping in axially-loaded notched strips for compliant building blocks. Smart Mater. Struct. 29 (2), 02LT03.
Zhao, Y., et al., 2020b. Employing TLBO and SCE for optimal prediction of the compressive strength of concrete. Smart Struct. Syst. 26 (6), 753–763.
Zhao, Y., et al., 2020c. A novel artificial bee colony algorithm for structural damage detection. Adv. Civ. Eng. 2020.
Zhao, Y., Zhong, X., Foong, L.K., 2021. Predicting the splitting tensile strength of concrete using an equilibrium optimization model. Steel and Composite Structures. Int. J. 39 (1), 81–93.
Zhao, Y., et al., 2022. Predicting compressive strength of manufactured-sand concrete using conventional and metaheuristic-tuned artificial neural network. Measurement 194, 110993.
Zuo, R., Carranza, E.J.M., 2011. Support vector machine: a tool for mapping mineral prospectivity. Comput. Geosci. 37 (12), 1967–1975.
Liu, Z., Zheng, J., Liu, W., Liu, X., Chen, Y., Ren, X.,... Lin, Z. (2020). Identification of the key host phases of Cr in fresh chromite ore processing residue (COPR). Sci. Total Environ. 703, 135075. doi: https://doi.org/10.1016/j.scitotenv.2019.135075.
Bai, B., Bai, F., Li, X., Nie, Q., Jia, X., Wu, H., 2022. The remediation efficiency of heavy metal pollutants in water by industrial red mud particle waste. Environ. Technol. Innov. 102944. https://doi.org/10.1016/j.eti.2022.102944.
Dai, L., Wang, Z., Guo, T., Hu, L., Chen, Y., Chen, C.,... Chen, J. (2022). Pollution characteristics and source analysis of microplastics in the Qiantang River in southeastern China. Chemosphere (Oxford), 293, 133576. doi: 10.1016/j.chemosphere.2022.133576.